Eur. Phys. J. C 41, 343–351 (2005)
Digital Object Identifier (DOI) 10.1140/epjc/s2005-02223-0

THE EUROPEAN PHYSICAL JOURNAL C

The unintegrated gluon distribution from the modified BK equation

K. Kutak[1,3,a], A.M. Staśto[2,3,4]

[1] II. Institut für Theoretische Physik, Universität Hamburg, Hamburg, Germany[b]
[2] Nuclear Theory Group, Brookhaven National Laboratory, Upton, NY 11973, USA[c]
[3] Institute of Nuclear Physics, Radzikowskiego 152, Kraków, Poland
[4] Theory Group, DESY, Notkestrasse 85, 22607 Hamburg, Germany

Received: 30 August 2004 / Revised version: 17 February 2005 /
Published online: 11 May 2005 –

Abstract. We investigate the recently proposed non-linear equation for the unintegrated gluon distribution function which includes the subleading effects at small x. We obtained numerically the solution to this equation in (x, k) space, and also the integrated gluon density. The subleading effects affect strongly the normalization and the x and k dependence of the gluon distribution. We show that the saturation scale $Q_s(x)$, which is obtained from this model, is consistent with the one used in the saturation model by Golec-Biernat and Wüsthoff. We also estimate the non-linear effects by looking at the relative normalization of the solutions to the linear and non-linear equations. It turns out that the differences are quite large even in the nominally dilute regime, that is when $Q^2 \gg Q_s^2$. Finally, we calculate the dipole–nucleon cross section.

1 Introduction

The knowledge of the QCD dynamics at high energies is essential in understanding the hadronic interactions studied at current (HERA, Tevatron) and future (LHC) accelerators. Parton distributions extracted from the HERA ep collider will be used in the description of the hadronic processes studied at LHC. It is very important to know these parton distributions with very high accuracy and, perhaps even more important, to be able to estimate possible uncertainties which may emerge when extrapolating to the kinematic regime of LHC. A lot of effort is currently devoted to extracting the parton distributions with very high precision [1,2] from the available experimental data.

In principle two different frameworks can be used for calculating the parton distributions. The standard one is based on the DGLAP evolution and collinear factorization. In the high energy limit it is also possible to use the k_T factorization [3] in which the QCD interaction is described in terms of the quantity which depends on the transverse momentum of the gluon i.e. the unintegrated gluon distribution. An equation which governs the evolution of this distribution is the BFKL equation [4]. Its well known solution leads to a very strong power growth of the gluon density with energy: $\sim s^\lambda$ where $\lambda = 4 \ln 2 \alpha_s N_c/\pi$ is the BFKL intercept in the leading logarithmic approximation in powers of $\alpha_s \ln 1/x$ (LLX). Next to leading order corrections to BFKL [5] decrease the rate of growth but do not change the power behavior of the gluon distribution. Thus the growth of the resulting hadronic cross section has to be eventually tamed in order to satisfy the unitarity bound [6].

The perturbative parton saturation, first discussed in a pioneering paper [7], is a phenomenon which slows down the rapid growth of the partonic densities. It is believed that it leads to the restoration of the unitarity of the scattering matrix[1]. When the density of gluons becomes very high, the gluon recombination has also to be taken into account. This leads to a modification of the evolution equations and their solution results in the saturation of the gluon density. In the high energy limit, the parton saturation is described by an infinite hierarchy of the coupled evolution equations for the correlators of Wilson lines [9]. It is equivalent to the JIMWLK functional equation [10] derived within the theory of the color glass condensate [11]. In the absence of correlations, the first equation in the Balitsky hierarchy decouples and is then equivalent to the equation derived independently by Kovchegov [12] within the dipole formalism [13].

It is desirable to have a formalism which embodies the resummation of the subleading corrections in $\ln 1/x$ and still contains the saturation effects. Various attempts in

[a] e-mail: kutak@mail.desy.de
[b] Permanent address.
[c] Permanent address.

[1] Unitarity or the Froissart bound is valid with respect to the whole QCD, whereas parton saturation is a perturbative mechanism. As discussed in [8], apart from the saturation, the confinement is also needed to satisfy the Froissart bound in QCD.

this direction already exist; see for example [14–23]. In this contribution we analyze in better detail the non-linear equation for the unintegrated gluon distribution function proposed in [19,20]. Its linear term is formulated within the unified BFKL/DGLAP framework [24] and the non-linear term is taken from the Balitsky–Kovchegov equation. We find that the subleading corrections play an important role in the calculation of the unintegrated gluon density since they reduce the value of the intercept and lower the overall normalization of the solution. We also study the differences of the solutions in the linear and non-linear case. It is interesting that these differences become amplified in the case of the integrated gluon density $xg(x,Q^2)$. The behavior of the saturation scale is controlled by the value close to the intercept of the solution of the linear equation. In our case this value is equal to the one suggested by HERA data, $Q_{\rm s} \sim \exp(\lambda Y)$ with $\lambda \simeq 0.3$. However, a more detailed analysis shows that even though saturation scale seems to be rather low, the actual numerical differences between the linear and non-linear solutions are much bigger. In other words, the effect of non-linearity on the overall normalization of the solution can be present already at the scales exceeding the saturation scale.

The outline of this paper is as follows: in the next section we introduce the Balitsky–Kovchegov equation and the formalism which enables to write it in terms of the unintegrated gluon distribution. In Sect. 3 we the recall basic ingredients of the unified BFKL/DGLAP framework and, following [19,20], we formulate the modified Balitsky–Kovchegov equation.

In Sect. 4 we perform a numerical analysis of this equation. We present its solution, i.e. the unintegrated gluon distribution as well as the integrated gluon density. Then, we perform the analysis of the saturation scale $Q_{\rm s}(x)$ and try to quantify the importance of the saturation effects by looking at the difference between the linear and non-linear solution. In Sect. 5 we present the results for the dipole cross section $\sigma(x,r)$ and compare them to the Golec-Biernat and Wüsthoff [25] parameterization. We summarize our study in the last section.

2 The Balitsky–Kovchegov equation

In the dipole picture [26] one can view the deep inelastic scattering process as a formation of the $q\bar{q}$ dipole, followed by the scattering of this dipole on the target. In the high energy, $s \gg Q^2 \gg \Lambda^2_{\rm QCD}$, regime these two processes are factorized, and the total $\gamma^* N$ cross section[2] can be written as

$$\sigma^{\gamma^* N}_{\rm T,L}(x,Q^2) = \int {\rm d}^2\mathbf{b}\, {\rm d}^2\mathbf{r}\, {\rm d}z\, |\Psi_{\rm T,L}(\mathbf{r},Q^2,z)|^2\, N(\mathbf{r},\mathbf{b},x)\ , \tag{1}$$

where $-Q^2 = q^2$ is the photon virtuality squared, and $x \simeq Q^2/s$ is the usual Bjorken variable. The quantity $\Psi_{\rm T,L}(\mathbf{r},Q^2,z)$ is the photon wave function which depends on the virtuality Q^2 and the size of the dipole $\mathbf{r}$, as well as the longitudinal fraction z of the photon momenta carried by the quark. The subscripts T and L denote the transverse and longitudinal polarization of the incoming photon, respectively. $N(\mathbf{r},\mathbf{b},x)$ is the amplitude for the scattering of the dipole at impact parameter $\mathbf{b}$ on the target. It contains all the information about the interaction of the dipole with the target.

The Balitsky–Kovchegov (BK) equation [9,12] is the non-linear equation for the amplitude $N(\mathbf{r},\mathbf{b},x)$

$$\begin{aligned}\frac{\partial N(\mathbf{r},\mathbf{b},x)}{\partial \ln 1/x} &= \overline{\alpha}_{\rm s} \int \frac{{\rm d}^2\mathbf{r}'\mathbf{r}^2}{(\mathbf{r}'+\mathbf{r})^2(\mathbf{r}')^2} \\ &\times \left[N\left(\mathbf{r}', \mathbf{b}+\frac{\mathbf{r}'+\mathbf{r}}{2}, x\right) + N\left(\mathbf{r}'+\mathbf{r}, \mathbf{b}+\frac{\mathbf{r}'}{2}, x\right)\right. \\ &-N(\mathbf{r},\mathbf{b},x) \\ &\left.- N\left(\mathbf{r}', \mathbf{b}+\frac{\mathbf{r}'+\mathbf{r}}{2}, x\right) N\left(\mathbf{r}'+\mathbf{r}, \mathbf{b}+\frac{\mathbf{r}'}{2}, x\right)\right],\end{aligned} \tag{2}$$

where $\overline{\alpha}_{\rm s} \equiv \frac{\alpha_{\rm s} N_{\rm c}}{\pi}$. The linear term on the right-hand side of (2) is equivalent to the BFKL equation in the coordinate space, whereas the non-linear term is responsible for the gluon recombination. It has been shown [40] to be equivalent to the triple pomeron vertex [41]. This equation has been independently derived in the dipole picture [12] and from Wilson's operator expansion [9]. In the latter case, (2) is just the first member of the infinite hierarchy which decouples in the absence of correlations.

In (2) there is a non-trivial interplay between the two sizes: the dipole size $\mathbf{r}$ and the impact parameter $\mathbf{b}$. The exact solution, recently studied in [27] (and in [28] with a modified kernel) has a very complicated $\mathbf{b}$ and $\mathbf{r}$ dependence which comes as a consequence of the conformal symmetry of this equation. Solutions to this equation simplified ignoring the impact parameter dependence have been extensively studied both analytically [29–31] and numerically [14,16,32–34]. Here we are interested in the unintegrated gluon density $f(x,k^2)$ averaged over the impact parameter $\mathbf{b}$. Following [19,20] we make the ansatz that this dependence factorizes:

$$N(\mathbf{r},\mathbf{b},x) = n(r,x)\, S(b)\ , \tag{3}$$

with the normalization conditions on a profile $S(b)$

$$\begin{aligned}\int {\rm d}^2\mathbf{b}\, S(b) &= 1\ , \\ \int {\rm d}^2\mathbf{b}\, S^2(b) &= \frac{1}{\pi R^2}\ ,\end{aligned} \tag{4}$$

where R is the target size in the impact parameter.

We are fully aware that the assumption (3) is crude, since it implies an approximation of an infinite and uniform target. To obtain the full $\mathbf{b}$ dependence one should consider the exact equation (2).

One can now transform (2) in the momentum space,

$$\Phi(\mathbf{l},\mathbf{b},x) = \int \frac{{\rm d}^2\mathbf{r}}{2\pi r^2}\, {\rm e}^{{\rm i}\mathbf{l}\mathbf{r}}\, N(\mathbf{r},\mathbf{b},x)\ , \tag{5}$$

[2] N being a target, nucleon or nucleus.

and taking

$$\Phi(\mathbf{l},\mathbf{b},x)=\phi(l,x)S(b)\ . \tag{6}$$

We neglect the angular dependence and assume that the functions n and ϕ depend only on the absolute values of $r\equiv|\mathbf{r}|$ and $l\equiv|\mathbf{l}|$. The relations (3), (5) and (6) enable one to write (2) in the following form [12]:

$$\frac{\partial\,\phi(l,x)}{\partial\,\ln 1/x}\ =\overline{\alpha}_{\rm s}\left[K\otimes\phi-\frac{1}{\pi R^2}\phi^2(l,x)\right]\ , \tag{7}$$

where we have integrated both sides of (2) over $\mathrm{d}^2\mathbf{b}$. Note that while $N(\mathbf{r},\mathbf{b},x)$ and $\Phi(\mathbf{l},\mathbf{b},x)$ are dimensionless, the functions $n(r,x)$ and $\phi(l,x)$ have dimension $\left[\frac{1}{\text{energy}^2}\right]$ due to the definitions (3) and (6). The operator K is the BFKL kernel [4] in momentum space in the LLx approximation. Let us now explicitly show how to find the relation between $\phi(l,x)$ and the unintegrated gluon distribution $f(x,k^2)$ defined through

$$xg(x,Q^2)\ \equiv\ \int^{Q^2}\frac{\mathrm{d}k^2}{k^2}\,f(x,k^2)\ , \tag{8}$$

with $xg(x,Q^2)$ being the integrated gluon density. The unintegrated gluon distribution is related to the dipole cross section

$$\sigma(r,x)=\frac{8\pi^2}{N_{\rm c}}\int\frac{\mathrm{d}k}{k^3}[1-J_0(kr)]\alpha_{\rm s}f(x,k^2)\ , \tag{9}$$

which in turn can be obtained from the amplitude $N(\mathbf{r},\mathbf{b},x)$ by performing the integration over $\mathbf{b}$:

$$\sigma(r,x)=2\int\mathrm{d}^2\mathbf{b}\,N(\mathbf{r},\mathbf{b},x)\,. \tag{10}$$

Using (5), (9) and (10) one obtains

$$\phi(l,x)=\frac{1}{2}\int\frac{\mathrm{d}^2\mathbf{r}}{2\pi r^2}\,\mathrm{e}^{\mathrm{i}\mathbf{l}\mathbf{r}}\,\frac{8\pi^2}{N_{\rm c}}\int\frac{\mathrm{d}k}{k^3}[1-J_0(kr)]\alpha_{\rm s}f(x,k^2)\ . \tag{11}$$

Integrating over angles yields

$$\begin{aligned}&\phi(l,x)\\&=\frac{2\pi^2}{N_{\rm c}}\int_{l^2}^{\infty}\frac{\mathrm{d}k^2}{k^4}\int_0^{\infty}\frac{\mathrm{d}r}{r}J_0(lr)[1-J_0(kr)]\alpha_{\rm s}f(x,k^2)\ ,\end{aligned} \tag{12}$$

and the integral over r gives

$$\phi(l,x)=\frac{\pi^2}{N_{\rm c}}\int_{l^2}^{\infty}\frac{\mathrm{d}k^2}{k^4}\ln\left(\frac{k^2}{l^2}\right)\alpha_{\rm s}f(x,k^2)\ . \tag{13}$$

Now we need to invert the operator

$$\hat{O}=\frac{\pi^2\alpha_{\rm s}}{N_{\rm c}}\int_{l^2}^{\infty}\frac{\mathrm{d}k^2}{k^4}\ln\left(\frac{k^2}{l^2}\right)g(k^2) \tag{14}$$

(where $g(k^2)$ is a test function), to get the expression for $f(x,k)$. Multiplying both sides of (12) by l^2 and performing the Mellin transform with respect to l^2 we obtain

$$\begin{aligned}\phi(\gamma,x)&\equiv\int\mathrm{d}l^2l^2\phi(l,x)(l^2)^{\gamma-1}\\&=\int\mathrm{d}l^2l^2\frac{\pi^2}{N_{\rm c}}\int_{l^2}^{\infty}\frac{\mathrm{d}k^2}{k^4}\ln\left(\frac{k^2}{l^2}\right)\alpha_{\rm s}f(x,k^2)(l^2)^{\gamma-1}\\&=\frac{\alpha_{\rm s}\pi^2}{N_{\rm c}}f(\gamma)\frac{1}{(\gamma+1)^2},\end{aligned} \tag{15}$$

and equivalently

$$f(\gamma)=\frac{N_{\rm c}}{\alpha_{\rm s}\pi^2}(\gamma+1)^2\phi(\gamma,x)\ . \tag{16}$$

The inverse Mellin transform gives

$$\begin{aligned}f(x,l^2)&=\frac{N_{\rm c}}{\alpha_{\rm s}\pi^2}\int\frac{\mathrm{d}\gamma}{2\pi\mathrm{i}}(l^2)^{-\gamma}(1+\gamma)^2\phi(\gamma,x)\\&=\frac{N_{\rm c}}{\alpha_{\rm s}\pi^2}\left(1-l^2\frac{\mathrm{d}}{\mathrm{d}l^2}\right)^2l^2\phi(l,x)\ .\end{aligned} \tag{17}$$

This relation between functions f and ϕ has been first derived in [32] and also in [19,20].

3 The non-linear equation for the unintegrated density

The relation (17) allows us to transform (7) into an equation for the unintegrated gluon distribution,

$$\begin{aligned}&\frac{\partial f(x,k^2)}{\partial\ln 1/x}=\frac{\alpha_{\rm s}N_{\rm c}}{\pi}\,k^2\int_{k_0^2}\frac{\mathrm{d}k'^2}{k'^2}\\&\times\left\{\frac{f\left(x,k'^2\right)-f\left(x,k^2\right)}{|k'^2-k^2|}+\frac{f\left(x,k^2\right)}{\left[4k'^4+k^4\right]^{\frac{1}{2}}}\right\}\\&-\alpha_{\rm s}\left(1-k^2\frac{\mathrm{d}}{\mathrm{d}k^2}\right)^2\frac{k^2}{R^2}\left[\int_{k^2}^{\infty}\frac{\mathrm{d}k'^2}{k'^4}\ln\left(\frac{k'^2}{k^2}\right)f(x,k'^2)\right]^2.\end{aligned} \tag{18}$$

It is BFKL equation supplemented by the negative non-linear term.

3.1 A partial resummation of the NLLx corrections

Equation (18) contains the BFKL kernel at leading logarithmic (LLx) accuracy. This is a coarse approximation as far as a description of the HERA data is concerned. It is well known [5] that the NLLx corrections to the BFKL equation are quite large. To make the equation more realistic, it was proposed [19,20] to implement in the linear term of (18) a unified BFKL-DGLAP framework developed in [24]. In this scheme [24], the BFKL kernel becomes modified by the consistency constraint [35,36]

$$k'^2\ <\ k^2/z\ , \tag{19}$$

imposed onto the real-emission part of the kernel in (18)

$$\int\frac{\mathrm{d}k'^2}{k'^2}\left\{\frac{f\left(\frac{x}{z},k'^2\right)\,\Theta\left(\frac{k^2}{z}-k'^2\right)\,-\,f\left(\frac{x}{z},k^2\right)}{|k'^2-k^2|}\right.$$

$$+\frac{f\left(\frac{x}{z},k^2\right)}{|4k'^4+k^4|^{\frac{1}{2}}}\Bigg\}\,. \tag{20}$$

The consistency constraint (19) resums a large part of the subleading corrections coming from a choice of scales in the BFKL kernel [37,38]. Additionally, the non-singular (in x) part of the leading order (LO) DGLAP splitting function is included into the evolution

$$\int_x^1\frac{\mathrm{d}z}{z}K\otimes f\rightarrow \tag{21}$$
$$\int_x^1\frac{\mathrm{d}z}{z}K\otimes f+\int^{k^2}\frac{\mathrm{d}k'^2}{k'^2}\int_x^1\mathrm{d}z\bar{P}_{gg}(z)f\left(\frac{x}{z},k'^2\right)\,,$$

where

$$\bar{P}_{gg}(z)=P_{gg}(z)-\frac{2N_{\mathrm{c}}}{z}\,. \tag{22}$$

Additionally, we assume that in our evolution equation α_{s} runs with scale k^2 which is yet another source of important NLLx corrections. The final improved non-linear equation for the unintegrated gluon density is as follows:

$$\begin{aligned}
f(x,k^2)&=\tilde{f}^{(0)}(x,k^2)\\
&+\frac{\alpha_{\mathrm{s}}(k^2)N_{\mathrm{c}}}{\pi}k^2\int_x^1\frac{\mathrm{d}z}{z}\int_{k_0^2}\frac{\mathrm{d}k'^2}{k'^2}\\
&\times\Bigg\{\frac{f\left(\frac{x}{z},k'^2\right)\,\Theta\left(\frac{k^2}{z}-k'^2\right)\,-\,f\left(\frac{x}{z},k^2\right)}{|k'^2-k^2|}\\
&\quad+\frac{f\left(\frac{x}{z},k^2\right)}{|4k'^4+k^4|^{\frac{1}{2}}}\Bigg\}\\
&+\frac{\alpha_{\mathrm{s}}(k^2)N_{\mathrm{c}}}{\pi}\int_x^1\mathrm{d}z\,\bar{P}_{gg}(z)\int_{k_0^2}^{k^2}\frac{\mathrm{d}k'^2}{k'^2}\,f\left(\frac{x}{z},k'^2\right)\\
&-\left(1-k^2\frac{\mathrm{d}}{\mathrm{d}k^2}\right)^2\frac{k^2}{R^2}\\
&\times\int_x^1\frac{\mathrm{d}z}{z}\left[\int_{k^2}^{\infty}\frac{\mathrm{d}k'^2}{k'^4}\alpha_{\mathrm{s}}(k'^2)\ln\left(\frac{k'^2}{k^2}\right)f(z,k'^2)\right]^2.
\end{aligned} \tag{23}$$

In [24] the inhomogeneous term was defined in terms of the integrated gluon distribution

$$\tilde{f}^{(0)}(x,k^2)=\frac{\alpha_S(k^2)}{2\pi}\int_x^1\mathrm{d}zP_{gg}(z)\frac{x}{z}g\left(\frac{x}{z},k_0^2\right) \tag{24}$$

taken at scale $k_0^2=1\,\mathrm{GeV}^2$. This scale was also used as a cutoff in the linear version of the evolution equation (23). In the linear case this provided a very good description of F_2 data with a minimal number of physically motivated parameters [24]. The initial integrated density at scale k_0^2 was parameterized as

$$xg(x,k_0^2)=N(1-x)^{\rho}\,, \tag{25}$$

where $N=1.57$ and $\rho=2.5$.

Let us finally note that in this model only the linear part of the BK equation has subleading corrections. We do not know yet how to include these corrections in the non-linear term. This would require the exact knowledge of the triple pomeron vertex [41] at NLLx accuracy, which is yet unknown beyond the LLx approximation.

4 Numerical analysis

4.1 The unintegrated and integrated gluon density

In this section we recall the method of solving (23) and we present the numerical results for the unintegrated gluon distribution function $f(x,k^2)$ and the integrated gluon density $xg(x,Q^2)$. The method of solving (23), developed in [20], relies on reducing it to an effective evolution equation in $\ln 1/x$ with the boundary condition at some moderately small value of x (i.e. $x=x_0\sim 0.01$).

To be specific, we make the following approximations. (1) The consistency constraint $\Theta(k^2/z-k'^2)$ in the BFKL kernel is replaced by the following effective (z independent) term

$$\Theta(k^2/z-k'^2)\rightarrow\Theta(k^2-k'^2)+\left(\frac{k^2}{k'^2}\right)^{\omega_{\mathrm{eff}}}\Theta(k'^2-k^2)\,. \tag{26}$$

This is motivated by the structure of the consistency constraint in the moment space, i.e.

$$\begin{aligned}
&\omega\int_0^1\frac{\mathrm{d}z}{z}z^{\omega}\Theta(k^2/z-k'^2)\\
&\quad=\Theta(k^2-k'^2)+\left(\frac{k^2}{k'^2}\right)^{\omega}\Theta(k'^2-k^2).
\end{aligned} \tag{27}$$

(2) The splitting function is approximated in the following way:

$$\begin{aligned}
&\int_x^1\frac{\mathrm{d}z}{z}[zP_{gg}(z)-2N_{\mathrm{c}}]f\left(\frac{x}{z},k'^2\right)\rightarrow\\
&\quad\bar{P}_{gg}(\omega=0)f(x,k'^2)\,,
\end{aligned} \tag{28}$$

where $\bar{P}_{gg}(\omega)$ is the moment function

$$\bar{P}_{gg}(\omega)=\int_0^1\frac{\mathrm{d}z}{z}z^{\omega}[zP_{gg}(z)-2N_{\mathrm{c}}]\,, \tag{29}$$

and

$$\bar{P}_{gg}(\omega=0)=-\frac{11}{12}\,. \tag{30}$$

This approximation corresponds to retaining only the leading term in the expansion of $\bar{P}_{gg}(\omega)$ around $\omega=0$ [39].

Using these approximations in (23) we obtain

$$\frac{\partial f(x,k^2)}{\partial \ln(1/x)} = \frac{\alpha_{\rm s}(k^2)N_{\rm c}}{\pi}\int_{k_0^2}\frac{{\rm d}k'^2}{k'^2}\left\{\frac{f\left(x,k'^2\right)\left[\Theta\left(k^2-k'^2\right)+\left(\frac{k^2}{k'^2}\right)^{\omega_{\rm eff}}\Theta\left(k^2-k'^2\right)\right]-f\left(x,k^2\right)}{|k'^2-k^2|}\right\}$$
$$+\frac{\alpha_{\rm s}(k^2)N_{\rm c}}{\pi}\bar{P}_{gg}(0)\int_{k_0^2}^{k^2}\frac{{\rm d}k'^2}{k'^2}f(x,k'^2)-\left(1-k^2\frac{\rm d}{{\rm d}k^2}\right)^2\frac{k^2}{R^2}\left[\int_{k^2}^{\infty}\frac{{\rm d}k'^2}{k'^4}\alpha_{\rm s}(k'^2)\ln\left(\frac{k'^2}{k^2}\right)f(x,k'^2)\right]^2 . \quad (31)$$

First, (31) was solved with the non-linear term neglected starting from the initial conditions at $x = 10^{-2}$ given by (24). The parameter $\omega_{\rm eff}$ was adjusted in such a way that the solution of the linear part of (31) matched the solution of the original equation in the BFKL/DGLAP framework [24]. This procedure gives $\omega_{\rm eff} = 0.2$ and the solution of the linear part of (31) reproduces the original results of [24] within 3% accuracy in the region $10^{-2} > x > 10^{-8}$ and $2\,{\rm GeV}^2 < k^2 < 10^6\,{\rm GeV}^2$. This matching procedure has also the advantage that the quark contribution present in the original BFKL/DGLAP framework is effectively included by fitting the value of $\omega_{\rm eff}$. The full non-linear equation (31) was then solved using the same initial conditions and setting $R = 4\,{\rm GeV}^{-1}$.

In Fig. 1 we plot the unintegrated gluon distribution function as a function of x for different values of k^2. This figure compares the results of two calculations, based on the linear and non-linear equations. The differences are not large, however there is some suppression due to the non-linearity at the smallest values, $x \leq 10^{-5}$.

The subleading corrections strongly decrease the value of the intercept with respect to the LLx value and the non-linear term becomes important only at very low values of x.

As is evident from Fig. 2 the subleading corrections cause a large suppression in the normalization, also at moderate values of x. This is due to the fact that the part of the P_{gg} splitting function non-singular in x was included into the evolution. This term is negative and is important at large and moderate values of x.

The same conclusions can be reached by investigating the plots in Fig. 3 where the unintegrated density is shown as a function of the transverse momentum k^2 for fixed values of x. The non-linear effects seem to have a moderate impact in that region. On the other hand the subleading corrections are substantial. For example, at $x = 10^{-5}$ and $k^2 = 10\,{\rm GeV}^2$ the reduction in magnitude of the unintegrated gluon density is about 25%.

In Fig. 4 we show the integrated gluon density given by (8). The change from the power behavior at small x is clearly visible in the non-linear case. Also the differences between the distributions in the linear and non-linear case seem to be more pronounced for the quantity $xg(x,Q^2)$. This is due to the fact that in order to obtain the gluon density $xg(x,Q^2)$ one needs to integrate over scales up to Q^2 including small values of k^2, where the suppression due to the non-linear term is bigger.

4.2 The saturation scale $Q_{\rm s}(x)$

In order to quantify the strength of the non-linear term, one introduces the saturation scale $Q_{\rm s}(x)$. It divides the space in (x,k^2) into regions of the dilute and dense partonic system. In the case when $k^2 < Q_{\rm s}^2(x)$ the solution of the non-linear BK equation exhibits the geometric scaling. This means that it is dependent only on one variable $N(r,x) = N(rQ_{\rm s}(x))$, or in momentum space $\phi(k,x) = \phi(k/Q_{\rm s}(x))$. Recently, an analysis of the saturation scale in the case of the model with resummed NLL BFKL has been performed [18]. There, the saturation scale was calculated from the formula

$$-\frac{{\rm d}\omega(\gamma_{\rm c})}{{\rm d}\gamma_{\rm c}} = \frac{\omega_{\rm s}(\gamma_{\rm c})}{1-\gamma_{\rm c}} , \quad (32)$$

which has been first derived in [7] by the boundary condition of the wave front. Formula (32) has been later rederived in [42,30]. The effective pomeron intercept $\omega_{\rm s}$ is a solution to the equation

$$\omega_{\rm s}(\gamma) = \bar{\alpha}_{\rm s}\,\chi(\gamma,\omega_{\rm s}) , \quad (33)$$

where $\chi(\gamma,\omega)$ is the kernel eigenvalue of the resummed model. In our case the eigenvalue has the following form:

$$\chi(\gamma,\omega) = 2\Psi(1) - \Psi(\gamma) - \Psi(1-\gamma+\omega) + \frac{\omega}{\gamma}\bar{P}_{gg}(\omega) . \quad (34)$$

The solution for the saturation scale obtained from solving (32,33) using eigenvalue (34) is shown in Fig. 5 and gives $\lambda = \frac{\omega_{\rm s}(\gamma_{\rm c})}{1-\gamma_{\rm c}} = 0.30, 0.45, 0.54$ for three values of $\alpha_{\rm s} = 0.1, 0.2, 0.3$, respectively. These results are similar to those obtained in [18]. We compare our results with the saturation scale from the Golec-Biernat and Wüsthoff model. Normalization of the saturation scale is set to match GBW saturation scale at $x_0 = 0.41 \times 10^{-4}$.

The saturation scale $Q_{\rm s}(x)$ can be also obtained directly from the numerical solution to the non-linear equation by locating, for example, the maximum of the momentum distribution of the unintegrated gluon density in the spirit of method presented in [14]. For the purpose of phenomenology we attempt here to estimate the effect of the non-linearity in a different, probably more quantitative way. We study the relative difference between the solutions to the linear and non-linear equations

$$\frac{|f^{\rm lin}(x,\tilde{Q}_{\rm s}(x,\beta)^2) - f^{\rm nonlin}(x,\tilde{Q}_{\rm s}(x,\beta)^2)|}{f^{\rm lin}(x,\tilde{Q}_{\rm s}(x,\beta)^2)} = \beta, \quad (35)$$

where β is a constant of order 0.1–0.5. Since this definition of the saturation scale is different from the one used in the

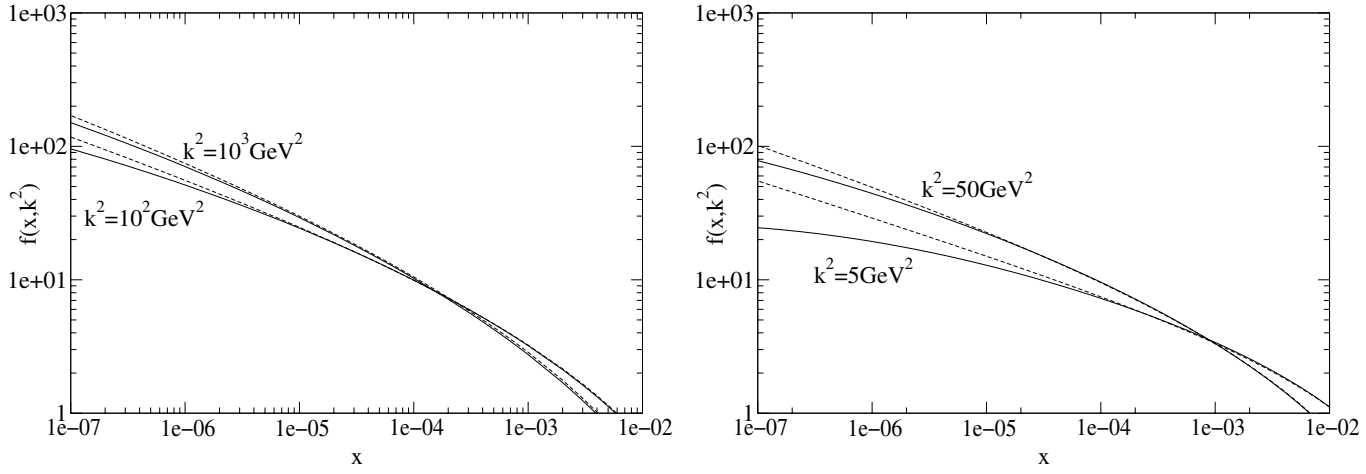

Fig. 1. The unintegrated gluon distribution $f(x, k^2)$ obtained from (31) as a function of x for different values $k^2 = 10^2\,\mathrm{GeV}^2$ and $k^2 = 10^3\,\mathrm{GeV}^2$ (left) and for $k^2 = 5\,\mathrm{GeV}^2$ and $k^2 = 50\,\mathrm{GeV}^2$ (right). The solid lines correspond to the solution of the non-linear equation (31) whereas the dashed lines correspond to the linear BFKL/DGLAP term in (31)

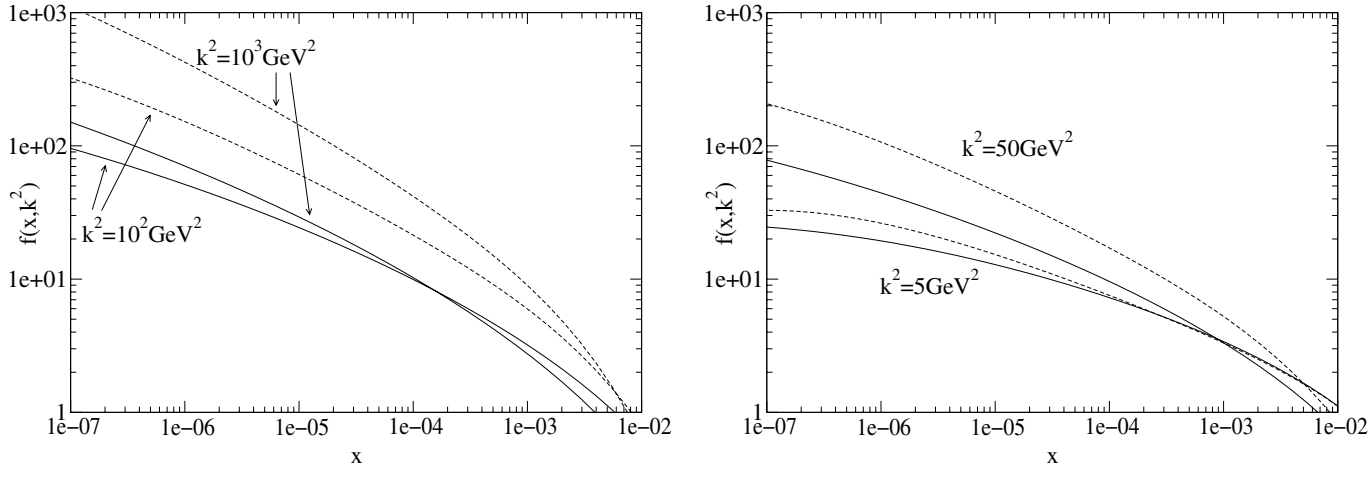

Fig. 2. The same as Fig. 1 but now the modified BK equation (31) (solid lines) is compared with the original BK equation (18) without subleading corrections (dashed lines)

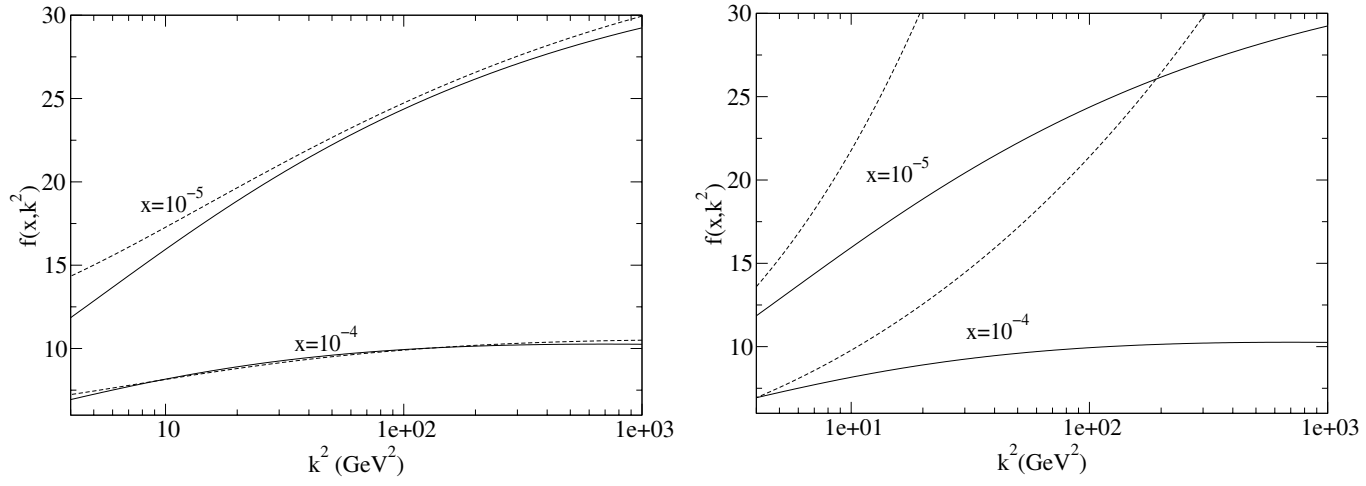

Fig. 3. The unintegrated gluon distribution $f(x, k^2)$ as a function of k^2 for two values of $x = 10^{-5}$ and 10^{-4}. Left: solid lines correspond to the solution of the non-linear equation (31) whereas dashed lines correspond to linear BFKL/DGLAP term in (31). Right: solid lines correspond to the solution of the non-linear equation (31) whereas dashed lines correspond to the solution of the original BK equation without the NLLx modifications in the linear part (18)

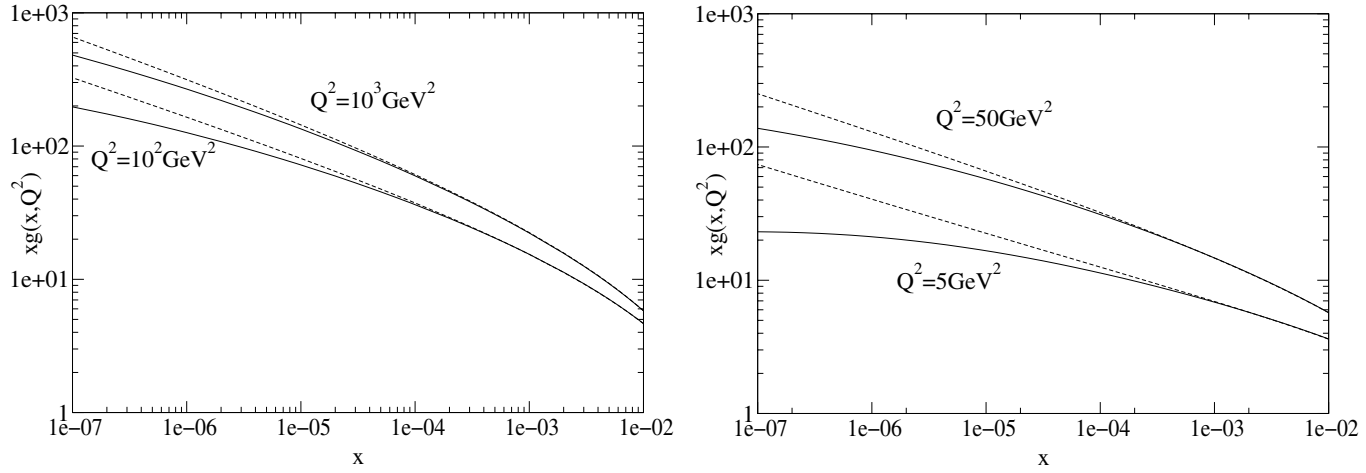

Fig. 4. The integrated gluon distribution $xg(x,k^2)$ as a function of x for values of $Q^2 = 10^2\,\mathrm{GeV}^2$ and $Q^2 = 10^3$ (left) and for $Q^2 = 5\,\mathrm{GeV}^2$ and $Q^2 = 50$ (right) obtained from integrating $f(x,k^2)$; see (31). Dashed lines correspond to solution of linear BFKL/DGLAP evolution equation

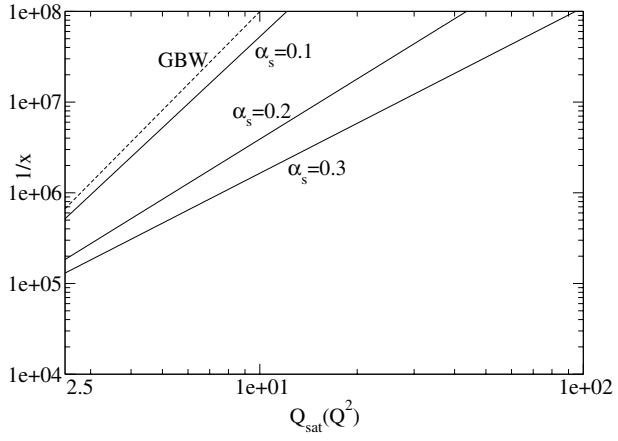

Fig. 5. Saturation scale obtained from (32) and (33) solid lines, compared with saturation scale from the GBW model [25]

literature and is likely to posses different x dependence, we denote it as $\tilde{Q}_\mathrm{s}$. In Fig. 6 (left) we show a set $\tilde{Q}_\mathrm{s}$ which are solutions to (35) for different choices of β together with the saturation scale calculated from the original saturation model by Golec-Biernat and Wüsthoff [25]. Solid lines given by (35) show where the non-linear solution for the unintegrated gluon starts to deviate from the linear one by $10\%, 20\%, \ldots, 50\%$. It is interesting that the contours $\tilde{Q}_\mathrm{s}(x)$ defined in (35) have much stronger x dependence than saturation scale $Q_\mathrm{s}(x)$ defined by (32) and the one from the GBW model. In particular $\tilde{Q}_\mathrm{s}(x,\beta) > Q_\mathrm{s}(x)$ for given x (at very small values of x). This might be a hint that saturation corrections can become important much earlier (i.e. for lower energies) than it would be expected from the usual definition of the saturation scale $Q_\mathrm{s}(x)$. In Fig. 6 (right) we also show contours in the case of the integrated gluon distribution function; that is, the solution to (35) with $f(x,k^2)$ replaced by $xg(x,Q^2)$. As already seen from the previous plot, see Fig. 4, the differences in the integrated gluon are more pronounced. For example in the case of $Q^2 = 25\,\mathrm{GeV}^2$ and $x \simeq 10^{-5}$–10^{-6} we expect about 15% to 30% difference in the normalization. Again, by looking solely at the position of the critical line, one would expect the non-linear effects to be completely negligible in this region since at $x = 10^{-6}$ the corresponding $Q_\mathrm{s}^2(x) \simeq 2.8\,\mathrm{GeV}^2$ (taking $Q_\mathrm{s}^2(x) = Q_{\mathrm{s},0}^2(x/x_0)^{-\lambda}$ with normalization $Q_{\mathrm{s},0}^2 = 1\,\mathrm{GeV}^2$ at $x_0 \simeq 4\times10^{-5}$ and $\lambda \simeq 0.28$, [25]). This rough analysis shows that one cannot think of the saturation scale as a definite and sharp border between a very dilute and a dense system. The transition between these two regimes appears to be rather smooth and the non-linear term of the equation seems to have quite a large impact on the normalization even in the "linear" regime defined as $Q^2 \gg Q_\mathrm{s}^2(x)$.

In practice, the estimate of the saturation effects is even more complicated since the unintegrated gluon density has to be convoluted with some impact factor, and the integration over the range of scales must be performed.

4.3 Dipole cross section $\sigma(r,x)$

It is interesting to see what is the behavior of the dipole cross section $\sigma(r,x)$ as obtained from the unintegrated gluon density via (9). In this calculation we assume that α_s is running with the scale k^2.

Calculation of the dipole cross section requires the knowledge of the unintegrated gluon density for all scales $0 < k^2 < \infty$. Since in our formulation the unintegrated gluon density is known for $k^2 > k_0^2$ we need to parameterize $f(x,k^2)$ for the lowest values of k^2, $k^2 < k_0^2$. We use the matching condition

$$xg(x,k_0^2) = \int_0^{k_0{}^2} \frac{\mathrm{d}k^2}{k^2} f(x,k^2)\,, \tag{36}$$

and following [43] we assume that $f(x,k^2) \sim k^4$ for low k^2. This gives (compare (25))

$$f(x,k^2) = 4N(1-x)^\rho k^4\,. \tag{37}$$

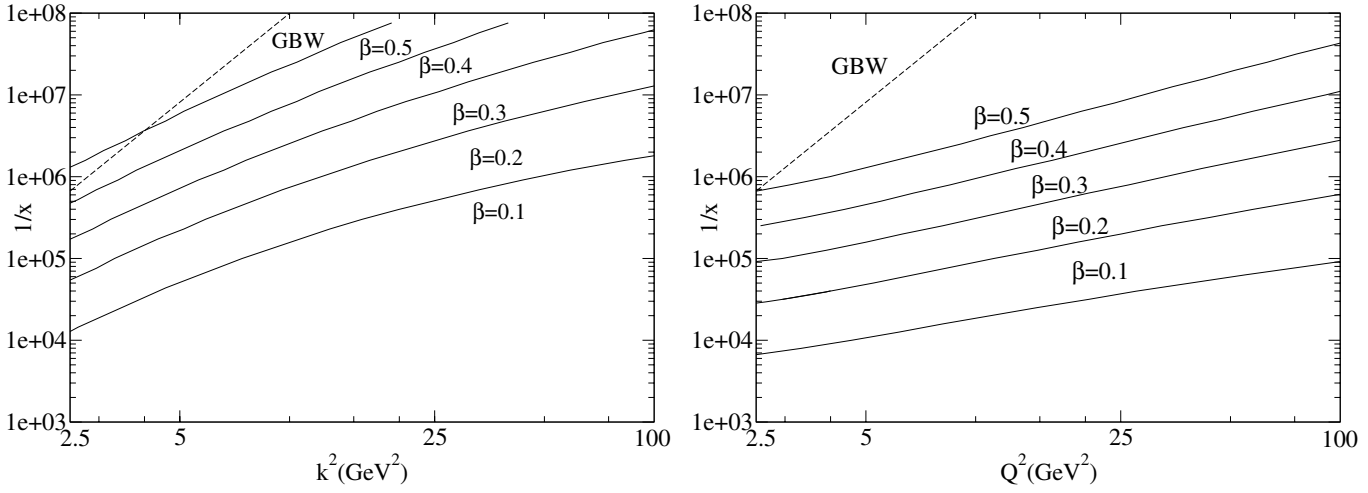

Fig. 6. Solid lines show contours of constant relative difference between solutions to linear and non-linear equations, (35). Lines from bottom to top correspond to 10%, 20%, 30%, 40%, 50% difference. Left: Contours in the case of the unintegrated gluon distribution $f(x,k^2)$; right: contours in the case of the integrated gluon distribution $xg(x,Q^2)$. A dashed line in both cases corresponds to the saturation scale from the Golec-Biernat and Wüsthoff model [25]

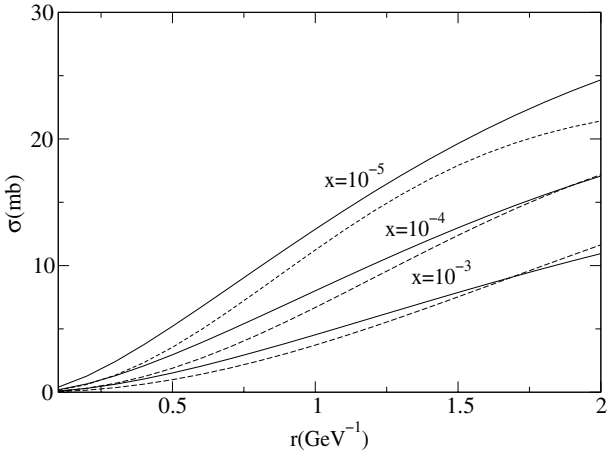

Fig. 7. The dipole cross section obtained from the modified BK (solid line) compared to the GBW dipole model (dashed line)

In Fig. 7 we present the dipole cross section as a function of the dipole size r for the three values of $x = 10^{-3}, 10^{-4}$ and 10^{-5}. For comparison we also present the dipole cross section obtained from GBW parameterization. To be self-consistent, we cut the plot at $r = 2\,\mathrm{GeV}^{-1}$ because we assumed in the derivation of formula (7) that the dipoles are small in comparison to the target size (we assume proton radius to be $4\,\mathrm{GeV}^{-1}$). This cut allows us to obtain a model independent result since we observe that different parameterizations of $f(x,k^2)$ for $k^2 < k_0^2$ give essentially the same contribution for $r < 2\,\mathrm{GeV}^{-1}$.

We observe that our extraction of the dipole cross section gives a similar result to the GBW parameterization. The small difference in the normalization is probably due to the different values of x_g which probe the gluon distribution (or alternatively the dipole cross section). In the GBW model the dipole cross section is taken at the value $x_g = x$ which is the standard Bjorken $x = Q^2/2p\cdot q$. On the other hand, in the formalism presented in [24] one takes into account the exact kinematics (energy conservation) in the photon impact factor. It is a part of the subleading effect in the impact factor and it increases the value of $x_g \sim 5x$. Therefore, in our formalism the normalization of the unintegrated gluon is increased so that the convolution with the impact factor and the resulting structure function remains the same.

5 Conclusions

In this paper we studied numerically the solutions to the modified BK equation in the approximation of the infinite and uniform target. The modifications include the subleading corrections in $\ln 1/x$ which are given by the kinematical constraint, DGLAP P_{gg} splitting function and the running of the strong coupling. Since these corrections reduce significantly the value of the BFKL intercept, they also have a large impact on the behavior of the saturation scale and the normalization of the solution. For example, we find that at $x = 10^{-4}$ and $k^2 = 100\,\mathrm{GeV}^2$ the normalization of the unintegrated gluon distribution is reduced by about 30%–40% as compared with the solution to the unmodified BK equation.

We have studied the onset of the non-linear corrections by observing the difference in the normalization of the linear and non-linear solutions. We observe that even though the solutions are in the nominally dilute regime, the normalization of the solution to the BK equation can be already strongly affected by the presence of the non-linear term. This can have potential impact on the extrapolation of the parton distributions to lower values of x. We note however that, as long as the non-linearities do not affect substantially the k and x dependence of the solution, the linear equation can probably be used with suitably chosen boundary conditions.

We have also computed the dipole cross section from this model and compared it with the GBW. We find that both models give similar results, with some small differences which can be atrributed to the slightly different treatment of the photon impact factor.

Finally, we stress that although the subleading corrections are included in this formalism by using the available knowledge on the NLLx BFKL equation and the resummation procedures, they are taken into account only in the linear part of the BK equation. A consistent and complete treatment would require their inclusion in the triple pomeron vertex part, which is so far known to LLx accuracy only.

Acknowledgements. We thank Jochen Bartels, Krzysztof Golec-Biernat, Hannes Jung, Misha Lublinsky, and Agustin Sabio-Vera for useful discussions. K.K. is supported by Graduiertenkolleg Zukünftige Entwicklungen in der Teilchenphysik. This research is partially supported by the U.S. Department of Energy Contract No. DE-AC02-98-CH10886 and by the Polish Committee for Scientific Research, KBN Grant No. 1 P03B 028 28.

References

1. A.D. Martin, R.G. Roberts, W.J. Stirling, R.S. Thorne, Eur. Phys. J. C **28**, 455 (2003); Eur. Phys. J. C **35**, 325 (2004)
2. J. Pumplin, D.R. Stump, J. Huston, H.L. Lai, P. Nadolsky, W.K. Tung, JHEP **0207**, 012 (2002)
3. S. Catani, M. Ciafaloni, F. Hautmann, Phys. Lett. B **242**, 97 (1990); Nucl. Phys. B **366**, 657 (1991)
4. L.N. Lipatov, Sov. J. Nucl. Phys. **23**, 338 (1976); E.A. Kuraev, L.N. Lipatov, V.S. Fadin, Sov. Phys. JETP **45**, 199 (1977); I.I. Balitsky, L.N. Lipatov, Sov. J. Nucl. Phys. **28**, 338 (1978)
5. V.S. Fadin, L.N. Lipatov, Phys. Lett. B **429**, 127 (1998); G. Camici, M. Ciafaloni, Phys. Lett. B **430**, 349 (1998)
6. M. Froissart, Phys. Rev. **123**, 1053 (1961)
7. L.V. Gribov, E.M. Levin, M.G. Ryskin, Phys. Rep. **100**, 1 (1983)
8. A. Kovner, U.A. Wiedemann, Phys. Rev. D **66**, 051502 (2002); D **66**, 034031 (2002); Phys. Lett. B **551**, 311 (2003)
9. I.I. Balitsky, Nucl. Phys. B **463**, 99 (1996); Phys. Rev. Lett. **81**, 2024 (1998); Phys. Rev. D **60**, 014020 (1999); Phys. Lett. B **518**, 235 (2001)
10. J. Jalilian-Marian, A. Kovner, A. Leonidov, H. Weigert, Nucl. Phys. B **504**, 415 (1997); Phys. Rev. D **59**, 014014 (1999).
    J. Jalilian-Marian, A. Kovner, H. Weigert, Phys. Rev. D **59**, 014015 (1999); E. Iancu, A. Leonidov, L. McLerran, Nucl. Phys. A **692**, 583 (2001)
11. L. McLerran, R. Venugopalan, Phys. Rev. D **49**, 2233 (1994); D **49**, 3352 (1994); D **50**, 2225 (1994); for a review see E. Iancu, R. Venugopalan, hep-ph/0303204
12. Yu.V. Kovchegov, Phys. Rev. D **60**, 034008 (1999)
13. A.H. Mueller, Nucl. Phys. B **415**, 373 (1994); Nucl. Phys. B **437**, 107 (1995)
14. K. Golec-Biernat, L. Motyka, A.M. Staśto, Phys. Rev. D **65**, 074037 (2002)
15. M.A. Braun, Phys. Lett. B **576**, 115 (2003)
16. M. Lublinsky, E. Gotsman, E. Levin, U. Maor, Nucl. Phys. A **696**, 851 (2001); M. Lublinsky, Eur. Phys. J. C **21**, 513 (2001)
17. D.N. Triantafyllopoulos, Nucl. Phys. B **648**, 293 (2003)
18. V.A. Khoze, A.D. Martin, M.G. Ryskin, W.J. Stirling, Phys. Rev. D **70**, 074013 (2004)
19. M.A. Kimber, J. Kwieciński, A.D. Martin, Phys. Lett. B **508**, 58 (2001)
20. K. Kutak, J. Kwieciński, Eur. Phys. J. C **29**, 521 (2003)
21. J.L. Albacete, N. Armesto, J.G. Milhano, C.A. Salgado, U.A. Wiedemann, Phys. Rev. D **71**, 014003 (2005)
22. G. Chachamis, M. Lublinsky, A. Sabio Vera, Nucl. Phys. A **748**, 649 (2005)
23. E. Gotsman, E. Levin, U. Maor, E. Naftali, hep-ph/0411242
24. J. Kwieciński, A.D. Martin, A.M. Staśto, Phys. Rev. D **56**, 3991 (1997); Acta Phys. Polon. B **28**, 2577 (1997)
25. K. Golec-Biernat, M. Wüsthoff, Phys. Rev. D **59**, 014017 (1999); D **60**, 114023 (1999); Eur. Phys. J. C **20**, 313 (2001)
26. N.N. Nikolaev, B.G. Zakharov, Z. Phys. C **49**, 607 (1991); Z. Phys. C **53**, 331 (1992)
27. K. Golec-Biernat, A.M. Staśto, Nucl. Phys. B **668**, 345 (2003)
28. E. Gotsman, M. Kozlov, E. Levin, U. Maor, E. Naftali, Nucl. Phys. A **742**, 55 (2004)
29. E. Levin, K. Tuchin, Nucl. Phys. B **573**, 833 (2000); Nucl. Phys. A **691**, 779 (2001)
30. S. Munier, R. Peschanski, Phys. Rev. Lett. **91**, 232001 (2003); Phys. Rev. D **69**, 034008 (2004); D **70**, 077503 (2004)
31. J. Bartels, V.S. Fadin, L.N. Lipatov, Nucl. Phys. B **698**, 255 (2004)
32. M.A. Braun, Eur. Phys. J. C **16**, 337 (2000); N. Armesto, M.A. Braun, Eur. Phys. J. C **20**, 517 (2001)
33. K. Rummukainen, H. Weigert, Nucl. Phys. A **739**, 183 (2004)
34. T. Ikeda, L. McLerran, hep-ph/0410345
35. B. Andersson, G. Gustafson, H. Kharraziha, J. Samuelsson, Z. Phys. C **71**, 613 (1996)
36. J. Kwieciński, A.D. Martin, P.J. Sutton, Z. Phys. C **71**, 585 (1996)
37. G.P. Salam, JHEP **9807**, 019 (1998); Acta Phys. Polon. B **30**, 3679 (1999)
38. M. Ciafaloni, D. Colferai, Phys. Lett. B **452**, 372 (1999); M. Ciafaloni, D. Colferai, G.P. Salam, Phys. Rev. D **60**, 114036 (1999)
39. J. Kwieciński, Z. Phys. C **29**, 561 (1985); R.K. Ellis, Z. Kunszt, E.M. Levin, Nucl. Phys. B **420**, 517 (1994); Erratum B **433**, 498 (1995); R.K. Ellis, F. Hautmann, B.R. Webber, Phys. Lett. B **348**, 582 (1995)
40. J. Bartels, L. Lipatov, G.P. Vacca, Nucl. Phys. B **706**, 391 (2005)
41. J. Bartels, Z. Phys. C **60**, 471 (1993); J. Bartels, M. Wüsthoff, Z. Phys. C **66**, 157 (1995); J. Bartels, C. Ewerz, JHEP **9909**, 026 (1999)
42. A.H. Mueller, D.N. Triantafyllopoulos, Nucl. Phys. B **640**, 331 (2003)
43. J. Bartels, K. Golec-Biernat, H. Kowalski, Phys. Rev. D **66**, 014001 (1999)